Molecular dynamics simulations of polymer transport in nanocomposites

Tapan Desai and Pawel Keblinski
Department of Material Science and Engineering, Rensselaer Polytechnic Institute, Troy, New York 12180

Sanat K. Kumar
Isermann Department of Chemical and Biological Engineering, Rensselaer Polytechnic Institute, Troy, New York 12180

(Received 7 April 2004; accepted 26 January 2005; published online 7 April 2005)

Molecular dynamics simulations on the Kremer–Grest bead-spring model of polymer melts are used to study the effect of spherical nanoparticles on chain diffusion. We find that chain diffusivity is enhanced relative to its bulk value when polymer-particle interactions are repulsive and is reduced when polymer-particle interactions are strongly attractive. In both cases chain diffusivity assumes its bulk value when the chain center of mass is about one radius of gyration R_g away from the particle surface. This behavior echoes the behavior of polymer melts confined between two flat surfaces, except in the limit of severe confinement where the surface influence on polymer mobility is more pronounced for flat surfaces. A particularly interesting fact is that, even though chain motion is strongly speeded up in the presence of repulsive boundaries, this effect can be reversed by pinning one isolated monomer onto the surface. This result strongly stresses the importance of properly specifying boundary conditions when the near surface dynamics of chains are studied. © *2005 American Institute of Physics*. [DOI: 10.1063/1.1874852]

I. INTRODUCTION

The dynamics of polymer melts and concentrated solutions in the bulk have been extensively studied both experimentally and by computer simulations.[1,2] For chain lengths shorter than the entanglement value, the self-diffusion coefficient D scales as $D \sim N^{-1}$, whereas for longer chains it is asymptotically expected to vary as $D \sim N^{-2}$. The issue of polymer mobility near interfaces is more complicated, since it may be expected to be strongly influenced by polymer-surface interactions and surface topography. While the dynamics of polymer melts near flat interfaces is relatively well understood,[3] polymer chain motion in nanocomposites was addressed only recently.[4–7] Several computational studies in this area shed light into the issue of glass transition temperature in nanoparticle filled melts, as well as the effect of surface interactions on melt diffusion and viscosity.[7,8] However, the majority of simulation studies of polymer melts with nanofiller were limited to short chains. Thus, there is hardly any separation of monomer-scale related structural features from the polymer-chain scale. In contrast, experiments on nanofilled polymers cover a broad range of the degree of polymerization and focus on systems where there is a clean separation of length scales.

In this paper we investigate the motion of model polymer melts composed of chains with a relatively high degree of polymerization ($N=80$) filled with solid nanoparticles using molecular dynamics simulations. The key questions that we address are the following: (i) What is the effect of polymer-particle interaction on the polymer and particle dynamics? (ii) What is the spatial extent of the influence of the particle surface on polymer chain mobility? (iii) Are the conformations and dynamics of the polymer chain different on curved and flat surfaces?

The paper is organized as follows. In Sec. II we describe the details of the simulation model and methods. In Sec. III A we examine the effect of polymer-nanoparticle interaction strength and particle volume fraction on polymer and nanoparticle diffusion. In Sec. III B we contrast these findings with polymer mobility on flat surfaces. Brief conclusions are presented in Sec. IV.

II. SIMULATION MODEL AND PROCEDURE

The molecular dynamics (MD) simulations employ the bead-spring polymer-chain model proposed by Kremer and Grest.[9–11] Interactions between all pairs of monomers are described by a purely repulsive potential derived by truncating and shifting a Lennard-Jones (LJ) potential at its minimum: $U(r)=4\varepsilon[(\sigma/r)^{12}-(\sigma/r)^{6}]+\varepsilon$ for $r<2^{1/6}\sigma$, and $U(r)=0$ for $r>2^{1/6}\sigma$. This potential is also known as the WCA potential.[12] All lengths are reported in units of σ. Adjacent bonded monomers interact via a stiff FENE potential,[13] which constrains the bond length to ~ 1. The combined effect of the LJ and FENE potentials prevents chains from crossing each other. In the majority of MD simulations, including those for the neat polymer and for polymers filled with nanoparticles, we considered 30 chains of length $N=80$ monomer units. We used a reduced polymer density $\rho^{*}=\rho\sigma^{3}=0.85$ where ρ is the monomer number density; this density corresponds to that of a dense melt. With these parameters, the edge size of the cubic simulation cell was ~ 14, which is about three times radius of gyration of the $N=80$ chain ($R_g \sim 4.7$). Periodic boundary conditions are employed in all three directions. To investigate possible finite size effects we performed several simulations for systems four times larger by volume (9600 monomers) with corresponding simulation box edge size $\sim 22(\sim 5R_g)$. A simple velocity

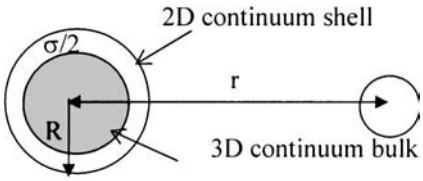

FIG. 1. Schematic representation of the interactions between a chain monomer and a nanoparticle. The interactions are divided into two parts, the outer 2D shell and inner 3D bulk.

rescaling thermostat is used to set the temperature $T=\varepsilon/k_B$, where k_B is Boltzmann's constant. Finally, in all simulations we used a MD time step equal to 0.005τ, where $\tau=(\varepsilon/m\sigma^2)^{1/2}$.

Nanoparticles were modeled as analytically smooth spheres of "LJ-continuum" (see Fig. 1). Each particle is comprised of an outer two-dimensional (2D) shell (of thickness $=0$) and an inner 3D bulk sphere region. The potential energy of interaction of a monomer with a particle is divided into two parts: the first originates from the inner 3D continuum sphere of radius 1.5, while the second is from an outer 2D continuum of radius $R=2$ and thickness$=0$ (see Appendix A). We follow the ideas of Steele and integrate the interactions between all particles in the particle and a chain monomer, and choose to use this model since it is computationally more efficient than considering a nanoparticle as a cluster of explicit atoms. Since the hard core radius of a monomer is ~ 0.5, the effective radius of the nanoparticle is $R=(2+0.5)=2.5$ (i.e., a diameter of $5\sim R_g$ of chains of length 80). The density of the interior 3D layer is $\rho_B\sigma^3=1.05$ which corresponds to the density of a crystalline, closed packed (fcc) arrangement of monomers. The density of the outer 2D shell is $\rho_s\sigma^2=0.94$, corresponding to the density of a (111) fcc plane.

Three types of nanoparticle-polymer interactions are studied, these are labeled as "repulsive," "attractive," and "strongly attractive," respectively. The repulsive particle involves only integrals of the repulsive part r^{-12} of the LJ potential. For computational simplicity we only kept the leading term of the integral over r^{-12}, which reproduces the complete integral for short monomer-particle separations and only causes minor errors at larger separations. The leading term for the repulsive potential, arising from the 2D continuum shell, is (see Appendix A for derivation)

$$U_{Nj}^{2Dr}=\frac{4\pi\varepsilon\rho_s\sigma^{12}R}{5r(r-R)^{10}}, \tag{1}$$

where r is the radial distance between the centers of the monomer and the nanoparticle. The leading term contribution from the 3D continuum bulk is

$$U_{Nj}^{3Dr}=\frac{4\pi\varepsilon\sigma^{12}\rho_B[9(R-\sigma/2)-r]}{360r[r-(R-\sigma/2)]^9}. \tag{2}$$

The total potential for a repulsive particle is the summation of the potentials from the 2D shell and 3D continuum, respectively.

The attractive particle involves integrals with the attractive r^{-6} of the LJ potential in addition to the repulsive contributions discussed above. We also kept just the leading term, which for the 2D continuum shell is

$$U_{Nj}^{2Da}=-\frac{4\pi\varepsilon\rho_s\sigma^6R}{2r(r-R)^4} \tag{3}$$

and the attractive part due to the 3D continuum bulk is

$$U_{Nj}^{3Da}=-\frac{4\pi\varepsilon\rho_B\sigma^6[3(R-\sigma/2)-r]}{12r[r-(R-\sigma/2)]^3}. \tag{4}$$

The total potential for the attractive particle model is the summation of all the 2D and 3D contributions, i.e., both repulsive and attractive parts. Finally, the potential for the strongly attractive particle is five times larger in magnitude than the potential for the attractive particle.

The structures are prepared by starting with low-density polymer melts with or without nanoparticles. We then gradually decrease the volume of the simulation cell, over several million MD steps, until the reduced density of 0.85 is reached. In the case of melts filled with nanoparticles, the melt density is kept constant by increasing the volume of simulation cell by the effective volume occupied by the nanoparticles. Consequently, in all our studies the hydrostatic pressure is equal to $\sim 15\varepsilon/\sigma^3$. In the next step we equilibrated all structures over a time interval such that each chain has moved at least $2R_g$. Such equilibrated structures are then used as starting structures for production runs of $(20-50)\times 10^6$ MD steps over which we collect structural and dynamical data.

In the majority of the simulations we place one nanoparticle at the center of the cubic simulation cell, i.e., we simulate a particle volume fraction of 2.5%. The particle volume fraction is varied by accommodating two particles (placed at the bcc sites of the cubic simulation cell) or with four particles (placed at the fcc sites) in a series of simulations. These last two cases correspond to particle volume fractions of 5% and 10%, respectively.

Initially, we fixed the positions of the nanoparticles. This leads, however, to unphysically high polymer chain diffusion. We deduce this as being caused by the fact that the interactions of polymer chains with stationary particles result in a net stochastic force acting on the center of mass of the polymer melt. This leads to a diffusive motion of the center of mass of the polymer melt, which is very significant for small system sizes involved in MD simulations. On the other hand, in real nanocomposites, the typical nanoparticles are 10–20 nm in size, and thus much heavier than the polymer chains. Consequently they can be considered to be stationary. Therefore, to be able to mimic this condition, we simulated stationary particles. However, we use a corrective procedure to eliminate the center of mass motion of the polymer melt. We calculate the total force acting on the polymer melt by the stationary nanoparticles at each time step. We then apply an equal and opposite force uniformly distributed over all monomers. For several cases we ran simulations with mobile particles without any correcting forces and obtained the same chain diffusion coefficients as with the corrected immobile

particle simulations. To test for the role of mass of the particles when they were mobile we considered two cases. In the first case, since the radius of the nanoparticle is five times larger than that of a monomer, its mass was chosen to be $5^3=125$ times greater. In the second case the nanoparticle is four times heavier than the former.

Systems involving flat surfaces consist of polymer melts sandwiched between two plates which are modeled, akin to the nanoparticles, as consisting of a 2D continuum surface and a 3D semi-infinite bulk LJ continuum. The associated potential was obtained by analytical integration, but it can also be obtained by taking the limit where the nanoparticle radius approaches infinity. For flat surface systems we also studied cases where either the ends of several polymer chains or just several $N=1$ monomers were grafted to the surface. In this case it was important to remove the net force acting on the polymer melt, in the same manner as for stationary particles, to eliminate spurious effects of the center of mass movement. Systems with flat surfaces are periodic in the two in-plane directions.

III. RESULTS

A. Nanoparticle-polymer system

1. Chain structure

We first analyze the structural characteristics relevant to chain immobilization at particle surfaces. Figure 2(a) shows the nanoparticle-monomer radial distribution function $g(r)$ for all three interaction types, repulsive, attractive, and strongly attractive. The corresponding potentials of mean force $W/k_BT=-\ln g(r)$ are shown in Fig. 2(b). As seen from Fig. 2, increasing attraction leads to a more pronounced layering of monomers at the particle surface. There is also an increase in the potential barrier, which is characterized as the energy required for monomer exchange from the first to the second shell. The potential barrier for attractive and repulsive particles is $\sim 2k_BT$ and $1k_BT$, respectively. In contrast, the barrier for the strongly attractive particle is $\sim 5k_BT$.

This large potential barrier translates into more pronounced monomer trapping at the particle surface. We characterized the trapping time by considering the total number of monomer entries from the second shell to the first shell as a function of time, and found that the repulsive and the attractive particles behave in essentially the same manner in this context. However, the strongly attractive particle yields about five times longer monomer residence times in the first shell. Based on this result we only considered the repulsive and strongly attractive particles in the diffusion studies, as the dynamics involving attractive particles is very similar to that of the repulsive particles.

2. Chain diffusion in the presence of isolated filler

To measure the diffusion coefficient of the chains we ran the systems typically up to times of $100\,000\tau$, and analyzed the mean square displacement of the center of mass of chains:[13]

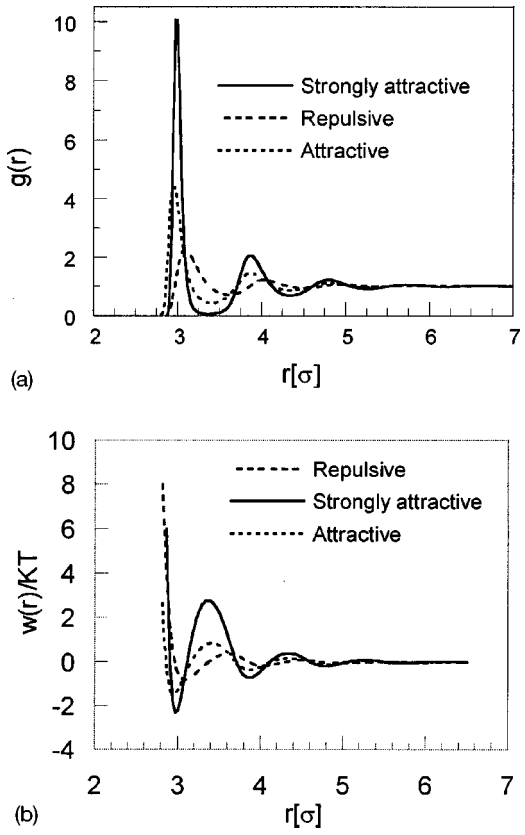

FIG. 2. (a) The particle-monomer radial distribution function $g(r)$ as a function of radial distance for repulsive, attractive, and strongly attractive system, respectively. Molecular layering is observed in all cases, and is most pronounced for the strongly attractive system. (b) The potential of mean force $W(r)/k_BT$ as a function of r for repulsive, attractive, and strongly attractive systems. The potential barrier for movement between first and second shells is significantly larger than the thermal energy for strongly attractive systems.

$$g_3(t) = \langle [r_{\text{c.m.}}(t_2) - r_{\text{c.m.}}(t_1)]^2 \rangle, \tag{5}$$

where $t=t_2-t_1$ and the outer brackets denote averaging over time and all chains in the system. The diffusion coefficient D results from the application of the Einstein equation: $g_3(t)=6Dt$. In Fig. 3, we show $g_3(t)$ for the neat melt and melts with a single repulsive and a strongly attractive particle, respectively. The self-diffusion coefficient for a neat system of

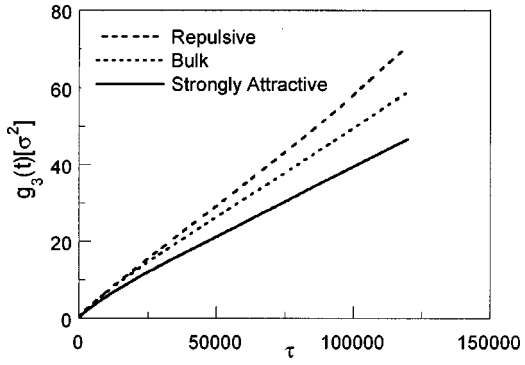

FIG. 3. Center of mass diffusion $g_3(t)$, averaged over all chains, as a function of time for the neat polymer (bulk) and for nanofilled systems. The long-time slope of this graph gives us the diffusion coefficient D. The value of D is highest for the repulsive nanoparticles, followed successively by the melt and the strongly attractive particle system.

chains of length $N=80$ is $(D\tau/\sigma^2)=(2.85\pm0.1)\times10^{-3}$. The presence of a repulsive nanoparticle results in the enhancement of the motion of chains, and the strongly attractive nanoparticle decreases their mobility. While the lower chain diffusion due to immobilization of chains induced by the particle-polymer attraction is expected, increased diffusion with repulsive surfaces is less obvious. We also note that, since our surfaces are analytically smooth, the chains can slide along them with no energy penalty ("slip" boundary condition). This enhanced diffusivity appears to be consistent with results of recent experiments[14] and simulations[15] where it was demonstrated that weakly bonding or repulsive interfaces leads to a lowering of the viscosity with respect to the neat system.

Our simulation cell size is only about factor of 3 larger than the polymer-chain radius of gyration. To assess finite size effects, we carried out simulations for a system with four nanoparticles and four times the volume of the former simulation box. The density was maintained at 0.85 and the volume fraction of nanoparticles at 2.5%. We performed two sets of simulations for systems with strongly attractive particles and repulsive particles. The diffusion coefficient in both cases was found to be within ±5% of the corresponding results obtained for the small box single nanoparticle simulations, suggesting that finite size effects probably play a minimal role in this context.

We now evaluate chain mobility as a function of distance from the particle surface to obtain a more detailed understanding of the observed diffusion behavior. We assign the dynamic properties of chains to spherical shells of thickness $R_g/3$ around the particle (recall that for $N=80$, $R_g=4.7$) according to the position of the chain center of mass at the time of origin, i.e., t_1 in Eq. (5). Thus, we monitor the mean square displacement (MSD) for each shell independently. We note that this procedure does not rigorously yield diffusion coefficients, since some chains will leave the shell before meaningful slopes from MSD can be obtained. However, the results are still indicative of the local chain diffusion coefficient.

In Fig. 4, we show the shell by shell value of the diffusion coefficient normalized by the value for the neat melt. Clearly, for the repulsive particle, the mobility near the nanoparticle surface is enhanced by about 20% over the bulk value. The distance required for the diffusion coefficient to reach its bulk value is $\sim R_g$. Strongly attractive particles reduce the mobility by roughly 40% near the particle surface, with bulklike behavior being recovered about an R_g from the surface.

3. Particle concentration effects on chain transport

The single particle simulations yielded overall diffusion coefficient changes of the order of 10% from the bulk value. In contrast, ~20%–40% changes are observed near the particle surface. To observe more pronounced changes in the overall diffusion coefficient we performed simulations with two and four nanoparticles in the simulation box, i.e., particle volume fractions of 5% and 10%, respectively. As shown in Fig. 5 for the particle volume fraction of 10%, the average chain diffusion coefficient is reduced by a factor of 2

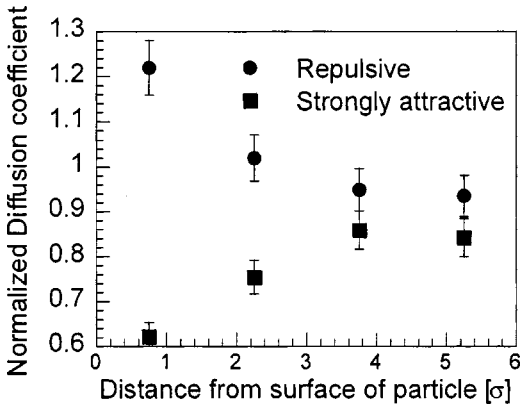

FIG. 4. The local diffusion coefficient D, normalized to the bulk value, as a function of r. For the repulsive particle the diffusion coefficient is highest at the surface. It gradually decreases to the bulk value. Similarly, the diffusion coefficient near the surface is lowest for strongly attractive particle indicating that the chains are less mobile. In both cases the bulk value is recovered $\sim R_g$ away from the particle surface.

with a strongly attractive particle. Even more interesting is the case of repulsive particles, where the diffusion coefficient initially increases with increasing particle concentration, but then it reaches a maximum and decreases with further increases in particle concentration. Our results appear to suggest that, while the initial particle concentration dependence of the diffusion coefficient reflects polymer-particle interactions, higher concentrations always lead to a reduction of the diffusion coefficient. We surmise that this might arise from simply geometrical reasons where diffusion eventually becomes strongly affected by the presence of tortuous paths in systems with large filler concentrations.

We note that all observed changes in the diffusion are purely dynamical in the sense that the conformation of the polymer chains remains essentially unchanged[16–19] as demonstrated in Tables I and II, where we list the radius of gyration for neat systems and for a number of filled systems with repulsive and attractive interactions and a range of volume fractions. Our results are a bit surprising that even at 10% volume fraction, where the particle-particle, surface-to-surface separation is equal to only one R_g, the polymers are not squeezed. This result is, however, consistent with the

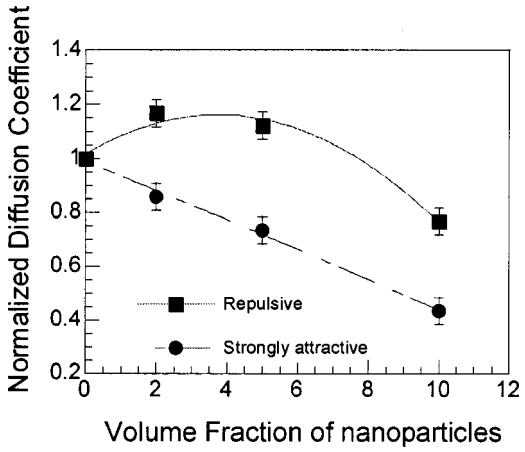

FIG. 5. The normalized overall diffusion coefficient as a function of volume fraction of nanoparticles for the repulsive and the strongly attractive system.

TABLE I. Comparison of radius of gyration R_g for systems with and without repulsive nanoparticles for different chain lengths N at 2.5% volume fraction of nanoparticles.

	Radius of gyration (R_g)	
Chain length (N)	Neat system	Repulsive
10	1.478±0.002	1.477±0.003
20	2.21±0.01	2.21±0.01
30	2.77±0.02	2.77±0.01
40	3.29±0.03	3.22±0.02
60	4.05±0.02	4.04±0.01
80	4.69±0.05	4.68±0.05
120	5.85±0.08	5.72±0.1

recent findings of Vacatello *et al.*[16] and is rationalized by the well known fact that the polymer coil obeys Gaussian coil statistics only in a time averaged manner. At any given instant the polymer assumes an elliptical shape, with the ratio of the longest to the shortest semiaxis equal to about 10.[20] So as is the case with flat surfaces,[21] instead of squeezing and changing shape, elliptical coils reorient themselves near or between particles, thus preserving their overall size even under strong confinement.

4. Particle transport

We also investigated how the interactions affect nanoparticle diffusion. For these studies, as described in Sec. II, particles were mobile and assigned with a mass either 125 times the mass of monomer (i.e., mass proportional to volume) or 500 times the mass of monomer. We are motivated to study the mass dependence since the ideas embodied in the Stokes equation would imply that the mass of the particle should be an irrelevant variable in this context, i.e.,

$$D = \frac{k_B T}{d\eta}, \tag{6}$$

where η is the viscosity of the embedding medium and d is the diameter of the sphere diffusing in the fluid. The diffusion coefficient was obtained in a similar manner as for chains, from the slope of the $g_3(t)$ [see Eq. (5)] of the particle as function of time, which was averaged over the entire simulation run of 20×10^6 MD steps. According to Table III,

TABLE II. Comparison of the radius of gyration R_g for systems containing repulsive and strongly attractive nanoparticles for different chain lengths N at 5% and 10% volume fraction of nanoparticles. There was no appreciable change found in the radius of gyration of polymer chains even at high nanoparticle concentration.

		Radius of gyration (R_g)	
	Chain length (N)	5% volume fraction	10% volume fraction
Strongly attractive particle	60	4.02±0.04	4.04±0.04
	80	4.57±0.05	4.69±0.05
	120	5.86±0.1	5.79±0.1
Repulsive particle	80	4.67±0.05	4.69±0.05

TABLE III. The diffusion coefficient of chains and the nanoparticle for strongly attractive nanoparticle and repulsive nanoparticle systems containing heavy, light, and stationary nanoparticles.

		Diffusion coefficient (σ^2/τ)1000		
		Heavy	Light	Stationary
Repulsive particle	Chains	3.3±0.2	3.1±0.2	3.3±0.2
	Particle	4.5±0.2	7.2±0.4	0.00
Strongly attractive particle	Chains	2.7±0.2	2.7±0.25	2.4±0.2
	Particle	0.43±0.05	0.7±0.05	0.00

the particle diffusion coefficient is actually higher than for the embedding $N=80$ chains in the case of the repulsive interactions. This is an expected result considering that the particle has about the same volume as a polymer chain, but it is much more compact and not entangled.

For the strongly attractive particle the diffusion coefficient is ten times smaller than of the repulsive particle. This dramatic decrease is associated with the formation of the "cage" of immobilized chains around the particle. Interestingly, the mobility of chains even at the particle surface is different only by about a factor of 2 for repulsive and attractive particles. In view of this, the behavior of the particle can be viewed as reflecting a collective sluggish effect, which is much more pronounced in comparison with the reduced mobility of individual chains.

Another interesting observation is that the particle self-diffusion coefficient depends on the particle mass, for both repulsive and attractive polymer-particle interactions, and is larger for the lighter particle. According to Eq. (6) the particle diffusivity should be mass independent. The underlying assumption of the validity of Eq. (6) is that the time scale associated with motions of particles in the medium is much smaller than the relaxation time scale of the Brownian motion of the particle. This is clearly not the case, as particle and polymer chains have similar masses and comparable diffusivities. In separate simulations of nanoparticle diffusion in a monomer melt ($N=1$) we observed, indeed, that the diffusivity of the nanoparticle is mass independent, as in this case there is good separation of time scales associated with monomer and nanoparticle motion. In both cases, we found the value of diffusion coefficient of the nanoparticle as $0.035\pm0.002(\sigma^2/\tau)$. Alder and co-workers[22] showed that the mutual diffusion coefficient is mass dependent, and it increases with increasing mass for similar size particles. Our simulations involve diffusion of a large particle, which is the case in Brownian motion described by Eq. (6).

B. Thin films

In the simulations described in the preceding section we studied the motion of polymer chains in the presence of nanoparticles. The sizes of the particles are comparable to the polymer R_g. A natural question is if the particle curvature plays an important role. To address this issue we studied

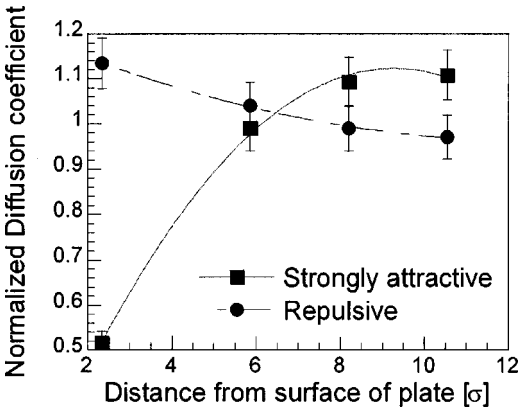

FIG. 6. The normalized diffusion coefficient as a function of distance from a flat surface for repulsive and attractive surfaces. The first shell, nearest to the surface, has a width of R_g, while all other shells have a width of $0.5R_g$.

polymer melts confined between two flat surfaces, at the same density and temperature as in the case of particle filled systems.

Figure 6 shows polymer-chain diffusivity as a function of position for the case of chains confined between two repulsive plates. As in the case of spherical particles, the diffusivity is enhanced ~15% near the surface and reaches its bulk value $\sim 1.2R_g$ away from the surface.[23–25] Chains confined between strongly attractive plates exhibit a ~50% reduction of diffusivity near the surface. Similarly, the bulk mobility is attained about $1.6R_g$ away from the surface (see Fig. 7). As the plates are brought closer the diffusivity, even in the middle of the film, does not regain the bulk value and at the plate-to-plate distance of $1.5R_g$ there is no observable chain diffusivity (see Fig. 7).

We do not observe similar confinement induced "glassification" in systems with strongly attractive spherical particles, even with surface-to-surface distance of R_g (i.e., at 10% volume fraction of particles). This difference might originate from the fact that spherical particles do not confine the polymer as effectively as planar surfaces. In addition, due to curvature of the nanoparticles, the strength of the polymer-

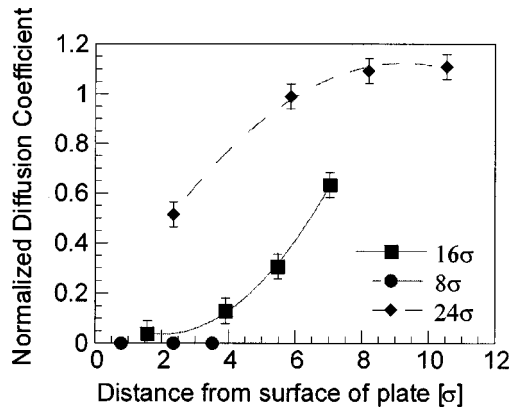

FIG. 7. The same as Fig. 6, but only for strongly attractive flat surfaces for various surface-to-surface distances. For the system in which surfaces are separated at a distance of 8 all the chains are immobilized due to confinement. The widths of the sampling shells for a plate separation of 24 is the same as for Fig. 6. For a plate separation of 16, the first shell has a width of $0.67R_g$, and the rest are $0.33R_g$ in thickness. For systems of thickness 8, the first and second shells are $0.33R_g$ in width and the third is $0.167R_g$.

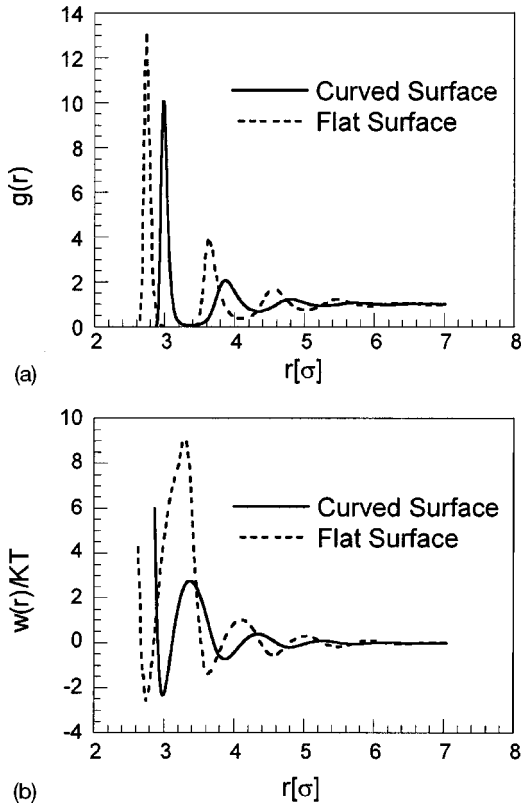

FIG. 8. (a) Comparing the particle-monomer radial distribution function $g(r)$ for nanoparticle and flat surface systems. Both cases correspond to strongly attractive surface polymer interactions. In the case of the flat plate the monomer distribution function is defined as a function of distance normal to the plates. Molecular layering is more pronounced for flat surfaces. The flat surface data are shifted by 1.8σ for better visualization. (b) Comparison of the potential of mean force $W(r)/k_BT$ as a function of radial distance for these two cases. The potential barrier for movement between the first and the second shells is almost three times larger for the flat surfaces.

surface attraction is larger for flat surfaces.[26] To illustrate this issue we compare the nanoparticle-monomer radial distribution function $g(r)$ for the strongly attractive nanoparticle system with a monomer distribution function in the direction normal to the flat strongly attractive plate [Fig. 8(a)]. The first peak for the flat surfaces is 30% higher than for the curved surfaces, substantiating this notion. The corresponding potential of mean force is shown in Fig. 8(b). The potential barrier for monomer exchange between the first and second shell is almost three times higher for the flat surfaces. (Note that the plot for the flat surface is shifted by 1.8 in the direction normal to the plate for better visualization.)

Finally, we explore the effect of the surface inhomogeneity and polymer grafting on the diffusion of unbonded chains. First we attached two isolated monomers to each flat surface through the use of FENE springs. The surface is repulsive to all chain monomers. As shown in Fig. 9, despite the low density of attached monomers, they essentially eliminate the enhanced diffusivity of chains in the vicinity of the surface. This might be associated with the fact that chain slippage on a smooth plane is arrested by the attached monomers, which act as obstacles. When, instead of monomers, two chains ends are grafted to each surface, the near surface diffusivity of nongrafted chains is reduced to almost half of its bulk value. However, it quickly recovers the bulk value as

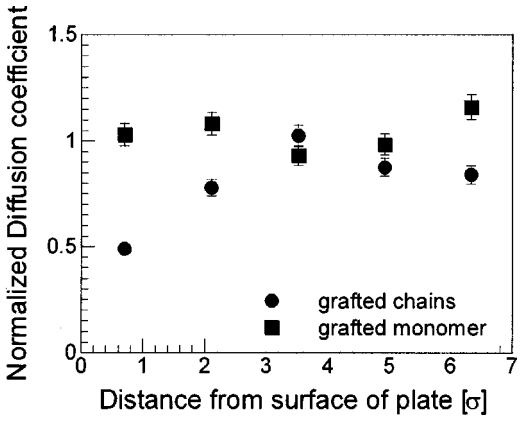

FIG. 9. The normalized diffusion coefficient as a function of distance from the plate surface for grafted polymeric chains and grafted monomers, respectively. The surfaces are repulsive to all monomers. The enhanced mobility due to repulsive interaction between plates and the chains near surface is reduced in both cases, with the effect being more pronounced for grafted chains. All shells are of a width $0.33R_g$.

one moves away from the surface. This indicates that the grafted chain end contributes more to the reduced chain diffusivity rather than the whole grafted chain.

IV. CONCLUSIONS

Our results clearly show that chain dimensions in filled systems are essentially equal to their unperturbed melt values even up to 10% by volume of filler. These results are in good agreement with the results of Vacatello[5] but not with the simulations of Mark's and Mattice's[18] research groups[17] and the experiments of Nakatani *et al.*[19] We consequently agree with Vacatello's conclusion that the calculations of Mark, which are for single RIS chains, may not properly account for the role of the high polymer density in real melts. The connection of our simulations to the experiments of Nakatani is unclear to us. We find that the role of confinement on chain motion is similar in the case of nanofilled polymers and for melts confined between two plates. The chain diffusivity is enhanced by 15%–20% near a repulsive surface and reduced by 40%–50% near a strongly attractive surface. The effect of confinement in strongly attractive nanofilled systems is not as strong as in the case of a melt between two plates, presumably due to geometrical reasons. However, we show that even subtle changes in the nature of polymer motion near a boundary (e.g., the introduction of a few pinned monomers) can cause qualitative changes to these results. Our conclusions therefore stress the importance of even subtle factors in determining the transport properties of polymers in filled polymer melts.

ACKNOWLEDGMENTS

The authors acknowledge the financial support of the Office of Naval Research, Contract No. N00014-01-10732, the National Science Foundation through Grant Nos. CMS-0310596 and DMR-0413755, and The National Science Foundation Nanoscale Science and Engineering Center at RPI, NSF Grant No. DMR-0117792. They thank Professor Sandy Sternstein for many useful discussions.

APPENDIX A: NANOPARTICLE-POLYMER INTERACTION POTENTIAL

The form of the interaction potential between a nanoparticle and a chain monomer is derived here. Figure 1 shows a schematic representation of the nanoparticle which consists of an inner 3D continuum core of a radius 1.5 and an outer 2D continuum shell of radius 2 (i.e., a 2D shell with thickness of 0). The procedure to obtain the integrated potential due to the $(\sigma/r)^{12}$ term from the 2D shell is the following: The potential is given by the integral over the shell,

$$U_{Nj}^{2Dr} = 4\varepsilon\rho_s \oint \frac{\sigma^{12}}{x^{12}} dA, \tag{A1}$$

where x is the distance between the monomer and a surface element on the shell, dA. The integral over the shell of thickness=0 can be performed in spherical coordinates by integrating over angles θ and ϕ. The integral over ϕ gives 2π, leading to,

$$U_{Nj}^{2Dr} = 4\varepsilon\rho_s\sigma^{12}2\pi R^2 \int_0^{\pi} \frac{-d\cos\theta}{(R^2+r^2-2Rr\cos\theta)^6}. \tag{A2}$$

Changing variables $\cos\theta = y$, we can simplify the integral in Eq. (A2),

$$U_{Nj}^{2Dr} = 4\varepsilon\rho_s\sigma^{12}2\pi R^2 \int_1^{-1} \frac{-dy}{(R^2+r^2-2Rry)^6}, \tag{A3}$$

which after straightforward integration gives,

$$U_{Nj}^{2Dr} = 4\varepsilon\rho_s\sigma^{12}2\pi R^2 \left[\frac{1}{10rR(r-R)^{10}} - \frac{1}{10rR(r+R)^{10}}\right], \tag{A4}$$

where r is the distance between the center of a nanoparticle and a chain monomer and R is the effective radius of the 2D shell. For simplicity, we only employ the first term in Eq. (A4) to represent the potential energy of interaction between a chain monomer and a repulsive nanoparticle. This only causes small errors at large r, while for small r it is almost precisely equal to the full Eq. (A4).

For the repulsive contribution from the 3D core we follow the same procedure as described above, again keeping only the leading term, and in addition integrating over the radial coordinate leading to Eq. (2). An analogous procedure is performed for the attractive parts of the potential, except, that the integrals over the 2D shell and the 3D core are done for the $-(\sigma/r)^6$ term, rather than for the $(\sigma/r)^{12}$ term.

[1] P. G. de Gennes, *Scaling Concepts in Polymer Physics* (Cornell University Press, Ithaca, 1985).
[2] M. Doi and S. F. Edwards, *The Theory of Polymer Dynamics* (Clarendon, Oxford, 1986).
[3] K. Binder, A. Milchev, and J. Baschnagel, Annu. Rev. Mater. Sci. **26**, 107 (1996).
[4] M. Vacatello, Macromolecules **34**, 1946 (2001).
[5] M. Vacatello, Macromolecules **36**, 3411 (2003).
[6] D. Brown, P. Mele, S. Marceau, and N. D. Alberola, Macromolecules **36**, 1395 (2003).
[7] G. D. Smith, D. Bedrov, L. Li, and O. Byutner, J. Chem. Phys. **117**, 9478 (2002).
[8] F. W. Starr, T. B. Schroder, and S. C. Glotzer, Macromolecules **35**, 4481 (2002).

[9]R. B. Bird, C. F. Curtiss, R. C. Armstrong, and O. Hassager, *Dynamics of Polymeric Liquids: Kinetic Theory* (Wiley, New York, 1987), Vol. 2.
[10]G. S. Grest and K. Kremer, Phys. Rev. A **33**, 3628 (1986).
[11]J. W. Rudisill and P. T. Cummings, Rheol. Acta **30**, 33 (1991).
[12]J. D. Weeks, D. Chandler, and H. C. Anderson, J. Chem. Phys. **54**, 5237 (1971).
[13]G. S. Grest and K. Kremer, J. Chem. Phys. **92**, 5057 (1990).
[14]M. E. Mackay, T. T. Dao, A. Tuteja, D. L. Ho, B. V. Horn, H.-C. Kim, and C. J. Hawker, Nat. Mater. **2**, 762 (2003).
[15]F. Varnik, J. Baschnagel, and K. Binder, Phys. Rev. E **65**, 021507 (2002).
[16]M. Vacatello, Macromolecules **35**, 8191 (2002).
[17]M. A. Saraf, A. Kloczkowski, and J. E. Mark, Comput. Theor. Polym. Sci., **11**, 251 (2001).
[18]W. E. Mattice (private communication).
[19]A. I. Nakatani, W. Chen, R. G. Schmidt, G. V. Gordon, and C. C. Han, Polymer **42**, 3713 (2001).
[20]J. Mazur, C. M. Guttmann, and F. L. McCrakin, Macromolecules **6**, 872 (1973)
[21]S. K. Kumar, M. Vacatello, and D. Y. Yoon, J. Chem. Phys. **89**, 5206 (1988).
[22]P. T. Herman and B. J. Alder, J. Chem. Phys. **56**, 987 (1972).
[23]P. A. Thompson, G. S. Grest, and M. O. Robbins, Phys. Rev. Lett. **68**, 3448 (1992).
[24]J. A. Torres, P. F. Nealey, and J. J. dePablo, Phys. Rev. Lett. **85**, 3221 (2000).
[25]T. S. Jain and J. J. dePablo, Macromolecules **35**, 2167 (2002).
[26]J. A. Baker, R. A. Pearson, and J. C. Berg, Langmuir **5**, 339 (1989).